



Dalton  
Transactions

**Methyldisulfide groups enable the direct connection of air-stable metal bis(terpyridine) complexes to gold surfaces**

Journal:	<i>Dalton Transactions</i>
Manuscript ID	DT-ART-03-2023-000955.R1
Article Type:	Paper
Date Submitted by the Author:	06-May-2023
Complete List of Authors:	Trang, Christina; University of Southern California Saal, Thomas; University of Southern California, Chemistry; University of Southern California Loker Hydrocarbon Research Institute, Inkpen , Michael ; University of Southern California,

SCHOLARONE™  
Manuscripts

# Methyldisulfide groups enable the direct connection of air-stable metal bis(terpyridine) complexes to gold surfaces

Christina D.M. Trang, Thomas Saal, and Michael S. Inkpen\*

*Department of Chemistry, University of Southern California, Los Angeles, CA 90089, United States*

E-mail: [inkpen@usc.edu](mailto:inkpen@usc.edu)

## ABSTRACT

We show that a new terpyridine ligand comprising a directly-connected methyldisulfide group (**tpySSMe**) can be used to prepare a modular series of metal bis(terpyridine) complexes,  $[M(\text{tpySSMe})_2](\text{PF}_6)_2$  ( $M = \text{Fe}, \text{Co}, \text{Zn}$ ), suitable for the functionalization of metal surfaces. Critically, we find these complexes are air-stable in solution for  $>7$  d, in stark contrast to their thiol-substituted analogues,  $[M(\text{tpySH})_2](\text{PF}_6)_2$  ( $M = \text{Fe}, \text{Co}$ ), which decompose in  $<1$  d. While **CoSH** has previously been utilized in several important studies, we explicitly detail its synthesis and characterization here for the first time. We subsequently probe the electrochemical properties of  $[M(\text{tpySSMe})_2](\text{PF}_6)_2$  in solution, showing that the (electro)chemical reactions associated with disulfide reduction significantly increase the complexity of the voltammetric response. In preliminary surface voltammetry studies, we confirm that **CoSS** and **FeSS** form solution-stable self-assembled monolayers (SAMs) on gold with comparable electrochemical properties to those formed from **CoSH**. Taken together, this work provides a robust foundation for future studies of this prominent class of complexes as redox-active components of SAMs or single-molecule junctions.

## INTRODUCTION

In seminal reports of unusual charge transport and magnetic phenomena, several studies have focused on self-assembled monolayers (SAMs) or molecular junctions comprising metal bis(terpyridine) complexes with *directly connected* sulfur-based anchors,  $[\mathbf{M}(\mathbf{L})_2]^{2+}$  (**Figure 1a**).  $[\mathbf{M}(\mathbf{L})_2]^{2+}$  complexes used include those with  $M = \text{Co}$ ,  $\text{Zn}$ , and  $\text{Ru}$ , where  $\mathbf{L}$  is  $\text{tpySAc} = 2,2':6',2''\text{-terpyridine-4'-thioacetate}$ ,  $\text{tpySH} = 2,2':6',2''\text{-terpyridine-4'-thiol}$ , or  $\text{tpy} = 2,2':6',2''\text{-terpyridine}$ .<sup>1-4</sup> In addition to their demonstrated utility, we also recognize that  $[\mathbf{M}(\mathbf{L})_2]^{2+}$  are potentially interesting redox-active molecular “platforms” – pre-formed components with bulky lateral dimensions that dictate the close-packed monolayer structure.<sup>3,5</sup> Such platforms may be used to introduce different functional species and/or free volume into a SAM without disrupting the underlying surface assembly process, a long-standing challenge in the field. Remarkably, however, no explicit synthetic procedures or characterization details for the aforementioned  $[\mathbf{M}(\mathbf{L})_2]^{2+}$  compounds are provided in the noted works or their referenced articles, significantly impeding further developments in this area.

We suggest that the direct attachment of anchor groups to pre-formed metal bis(terpyridine) monolayer components provides specific advantages for controlling the organization and composition of SAMs comprising these functional units. Previously reported surface attachment strategies using extended, pendant surface tethers<sup>6-10</sup> introduce additional degrees of freedom that can complicate molecular packing at the nanoscale.<sup>11,12</sup> While stepwise surface-based synthetic reactions have been utilized to construct similar complexes *in situ*,<sup>13-16</sup> here it may be challenging to control the extent to which different ligands and metals are introduced into such SAMs as a result of the varying kinetics of metal-ligand complexation and intramolecular steric effects within the surface layer.<sup>17-19</sup>

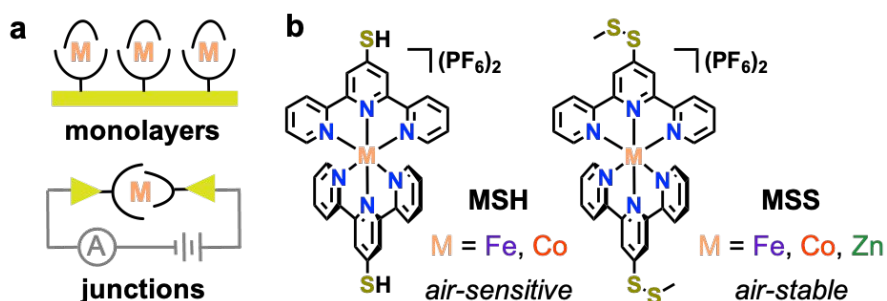


**Figure 1.** (a) Transition metal bis(terpyridine) complexes have been frequently targeted as modular components of self-assembled monolayers (SAMs) or molecular-scale junctions. (b) Molecular structures of  $[\text{M}(\text{tpySH})_2](\text{PF}_6)_2$  (**MSH**) and  $[\text{M}(\text{tpySSMe})_2](\text{PF}_6)_2$  (**MSS**).  $^1\text{H}$  NMR spectroscopic studies reveal **MSH** complexes are air-sensitive in solution, in contrast to their air-stable **MSS** analogues.

Potential challenges in resolving preparative methods for  $[\mathbf{M}(\mathbf{L})_2]^{2+}$  may be convoluted with the reported instabilities of related compounds in air. A detailed 2008 study of  $[\text{Fe}(\text{tpySH})_2](\text{PF}_6)_2$  (**FeSH**) found it was stable for only  $\sim 1$  d in solution, forming a tetrameric product through disulfide oxidation.<sup>20</sup> Deprotonation of **FeSH** was also shown by  $^1\text{H}$  NMR, UV-vis, and IR spectroscopy to produce a highly air-sensitive thione complex  $\text{Fe}(\text{tpy}=\text{S})_2$ .<sup>20</sup> Few characterized examples of other **tpySH**-containing metal bis(terpyridine) complexes (with  $\text{M} = \text{Ru}^{21}$  and  $\text{Ni}^{22}$ ) have been described. While thiol-protected ligands such as **tpySAc**<sup>23</sup> could offer routes to stable precursor complexes, deprotection of the corresponding  $[\text{M}(\text{tpySAc})_2](\text{PF}_6)_2$  complexes (e.g., with  $\text{NBu}_4\text{OH}$ ,  $\text{NBu}_4\text{F}$ ) is anticipated to result in unstable thione species via the intermediate thiolate. Such deprotection strategies are likely further complicated by counterion exchange by  $\text{OH}^-/\text{F}^-$ , or counterion loss from the charge neutral thione. New approaches are urgently needed to access air-stable  $[\mathbf{M}(\mathbf{L})_2]^{2+}$  complexes capable of binding to metal surfaces. In this work, we demonstrate that complexes comprising a new methyl-disulfide (-SSMe)-functionalized ligand (**MSS**;  $\text{M} = \text{Fe}, \text{Co}, \text{Zn}$ ) are both synthetically accessible and air-stable in solution, in stark contrast to **CoSH** which rapidly decomposes when exposed to air (**Figure 1b**). Preliminary surface voltammetry studies reveal **CoSS** forms solution-stable SAMs with comparable surface coverage and redox peak widths to **CoSH**, confirming that the -SSMe group serves as a competent anchor for binding these complexes to metal surfaces.

## RESULTS AND DISCUSSION

We explicitly target -SSMe groups as alternative, chemically robust, sulfur-based surface linkers for functional metal bis(terpyridine) complexes for several key reasons. Critically, Whitesides *et al.* have shown dialkyl-disulfides can spontaneously form SAMs of comparable composition to those constructed from analogous alkylthiols,<sup>24</sup> and it has recently been determined that disulfide groups cleave during solution-based scanning tunneling microscope-based break junction studies to form covalent gold-sulfur bonded single-molecule junctions.<sup>25</sup> We further reasoned that disulfides would exhibit good chemical compatibility with terpyridine coordination chemistry given the numerous examples of metal complexes comprising intact 4,4'-dipyridyl-disulfide ligands.<sup>26</sup> Use of an asymmetric disulfide, rather than a symmetric ligand such as **terpy-SS-terpy**,<sup>27</sup> would avoid the formation of coordination oligomers/polymers at homoleptic metal centers. We recognize that such asymmetrical disulfides will produce mixed SAMs containing dissociated, surface-bound -SMe, with

compositions that likely deviate from a 1:1 ratio.<sup>28</sup> However, we anticipate that domains of bound -SMe species would exhibit minimal stabilizing lateral interactions due to the short alkane component,<sup>28–30</sup> ensuring that the terpyridine complex is maximally competitive for surface binding. We also anticipate that any residual -SMe is small enough to bind within the area occupied by the complex on the surface. The practical utility of the -SSMe group in this context is evaluated below through surface voltammetry experiments.

We prepared the new ligand 4'-(methyl-disulfide)-2,2':6',2''-terpyridine (**tpySSMe**) in two steps from 4'-chloro-2,2':6',2''-terpyridine in 79% overall yield (**Figure 2a**). Our approach involved the formation of **tpySH** via nucleophilic attack by sodium hydrosulfide,<sup>27</sup> which is then methylthiolated using S-methyl methanethiosulfonate.<sup>31</sup> The X-ray crystal structure of this ligand is shown in **Figure 2b**. Following established methods,<sup>32–34</sup> reactions of **tpySSMe** with the appropriate M<sup>2+</sup> salt at room temperature provided the corresponding [M(**tpySSMe**)<sub>2</sub>](PF<sub>6</sub>)<sub>2</sub> complexes for M = Fe (**FeSS**), Co (**CoSS**), and Zn (**ZnSS**) (**Figure 2c**). <sup>1</sup>H NMR spectra reveal that **MSS** are stable in MeCN-d<sub>3</sub> solutions for ≥7 d, in stark contrast to the ~1 d reported for **FeSH** (see **SI, Figure S16** for representative **FeSS** spectra). For completeness, we obtained not only the <sup>1</sup>H NMR spectrum for the paramagnetic d<sup>7</sup> Co(II) **CoSS** complex,<sup>35</sup> but also the spectrum of the corresponding diamagnetic Co(III) d<sup>6</sup> species (**CoSS**<sup>3+</sup>) after chemical oxidization of **CoSS** with AgPF<sub>6</sub>. X-ray crystal structures of **FeSS**, **CoSS**, and **ZnSS** show the expected homoleptic metal complexes with distorted octahedral geometries and intact disulfide groups (**Figure 2d-f**). Small changes in the average 4'-carbon-4''-carbon distances of 9.256, 9.372, and 9.432 Å, respectively (denoted by † and ‡ for **FeSS**), correlate with the average M-N bond distances for each compound (Fe-N = 1.947(8), Co-N = 2.016(5), Zn-N = 2.152(4) Å). As expected, the structure and dimensions of these complexes are not appreciably altered by varying the central metal ion, an important consideration in the pursuit of well-mixed multicomponent SAMs.

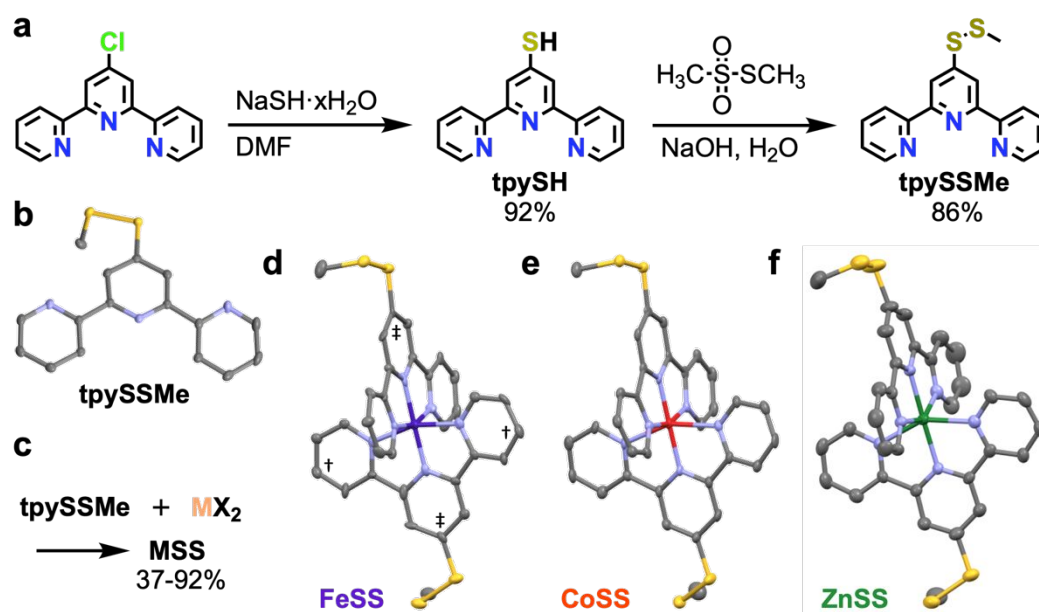


**Figure 2.** (a) Two-step synthetic route to **tpySSMe** ligand. (b) X-ray crystal structure of **tpySSMe**. (c) Synthetic route to disulfide-functionalized complexes (M = Fe, Co, Zn) using M<sup>2+</sup> salts (see the SI for detailed synthetic methods). (d-f) X-ray crystal structures of **FeSS**, **CoSS**, and **ZnSS**, respectively. Small changes in the average 4-carbon-4''-carbon distances (denoted by † and ‡ for **FeSS**) correlate with the average M-N bond distances for each compound. Hydrogen atoms, solvent, and counter ions (where relevant) are omitted from all crystal structures for clarity (50% probability ellipsoids, S = yellow, N = blue, C = grey, Fe = purple, Co = orange, Zn = green). Selected structural parameters are provided in the SI, Tables S1-8.

With routes to air-stable **MSS** complexes established, we sought to develop a robust synthesis of **CoSH** to determine whether this (in addition to **FeSH**) exhibits air-instability in solution. Following a method analogous to that used for **CoSS** (see the SI for detailed synthetic methods), the reaction of **CoCl<sub>2</sub>·6H<sub>2</sub>O** with **tpySH** under an inert nitrogen atmosphere initially provided an orange solution, but ultimately yielded a black solid with an intractable <sup>1</sup>H NMR spectrum after work up in air. Pure **CoSH** was isolated as a dark orange powder only with rigorous exclusion of air during synthesis and purification, as confirmed by <sup>1</sup>H NMR spectroscopy, mass spectrometry, and elemental analysis. Notably, this complex was observed to decompose in solution after air-exposure in <1 d, as indicated by significant changes in its paramagnetic <sup>1</sup>H NMR spectrum (SI, Figure S17). This clearly indicates that **MSH** (at least for M = Fe, Co) should only be utilized in SAMs or molecular junctions if these can be formed and studied under an inert atmosphere. While the -SH group that contacts the surface may be stabilized, in air the unbound -SH groups may form disulfide-linkages between adjacent molecules or form unstable thione-based complexes if exposed to basic environments (see

above discussion of **FeSH** solution stability). We note that performing solution-based molecular junction measurements with rigorous exclusion of air is not trivial, requiring custom-built instrumentation that is not yet widely available.<sup>36</sup>

We subsequently assessed the influence of the redox active -SSMe group<sup>37</sup> on the electrochemical properties and stability of **MSS** complexes in solution. In **Figure 3a-c** we plot overlaid solution cyclic voltammograms of **FeSS**, **CoSS**, and **ZnSS**, respectively. For potential windows that do not extend below approximately  $-1.4$  V vs. the FcH/[FcH]<sup>+</sup> redox couple, we find that both **FeSS** and **CoSS** show single reversible redox events ( $i_{pa}/i_{pc} \approx 1$ ,  $i_p \propto V_s^{1/2}$ ; selected data is provided in the **SI, Table S9**). We assign these features to the  $M^{2+/3+}$  couple, as their redox potentials align well with the same processes reported for the parent species (**SI, Figure S2, Table S9**). These solution studies indicate that SAMs comprising **FeSS** or **CoSS** may be unambiguously characterized by surface voltammetry at potentials positive of the disulfide, or anticipated gold-sulfur,<sup>38</sup> reduction processes, as we confirm below. **ZnSS** voltammograms are featureless across this potential range.

When the electrochemical window is extended to more reducing potentials, we observe a new irreversible reduction feature with a peak potential around  $-1.5$  V for all compounds. This feature is notably absent in voltammograms of the parent species (**Figure S2**), and significantly increases the complexity of the voltammetric response. Through comparison to voltammograms of the free **tpySSMe** ligand (**SI, Figure S3a and Table S10**), and other aspects of the **MSS** voltammograms (see below), we tentatively attribute this feature to the 1 or 2 e<sup>-</sup> reduction of a disulfide group. This process is thought to facilitate heterolytic or homolytic S-S bond cleavage, respectively, resulting in formation of the corresponding thiyl radical and/or thiolate species (i-a or i-b, **Figure 3e**).<sup>37,39,40</sup> In **MSS**, metal-coordination appears to increase the potential of disulfide reduction by approximately  $+0.7$  V (**SI, Table S10**). When scanning to even greater reducing potentials we observe additional features we attribute to the reversible ligand-based reductions previously assigned for  $[M(tpy)_2]^{2+}$ , now shifted to lower potentials as would be expected following the *in situ* generation of an electron-rich thiolate group.<sup>41</sup>

Any thiolate species formed from the reduction of a disulfide in **MSS** may be subsequently oxidized to thiyl radicals upon cycling back to more positive potentials. These radicals can then combine to form a mixture of symmetrical and asymmetrical disulfides (iii, **Figure 3e**).<sup>37</sup> Indeed, solution voltammograms that show disulfide reduction waves also exhibit new features between  $-0.3$  and  $0.9$  V that we attribute to thiolate oxidation processes (ii, **Figure 3a-c**). In **Figure S3**, we present solution voltammograms for **tpySSMe** and dimethyldisulfide

(MeSSMe) for comparison. The potentials for thiolate oxidation appear to be sensitive to the group bound to sulfur and the surrounding electrolytic environment (**Table S10**).

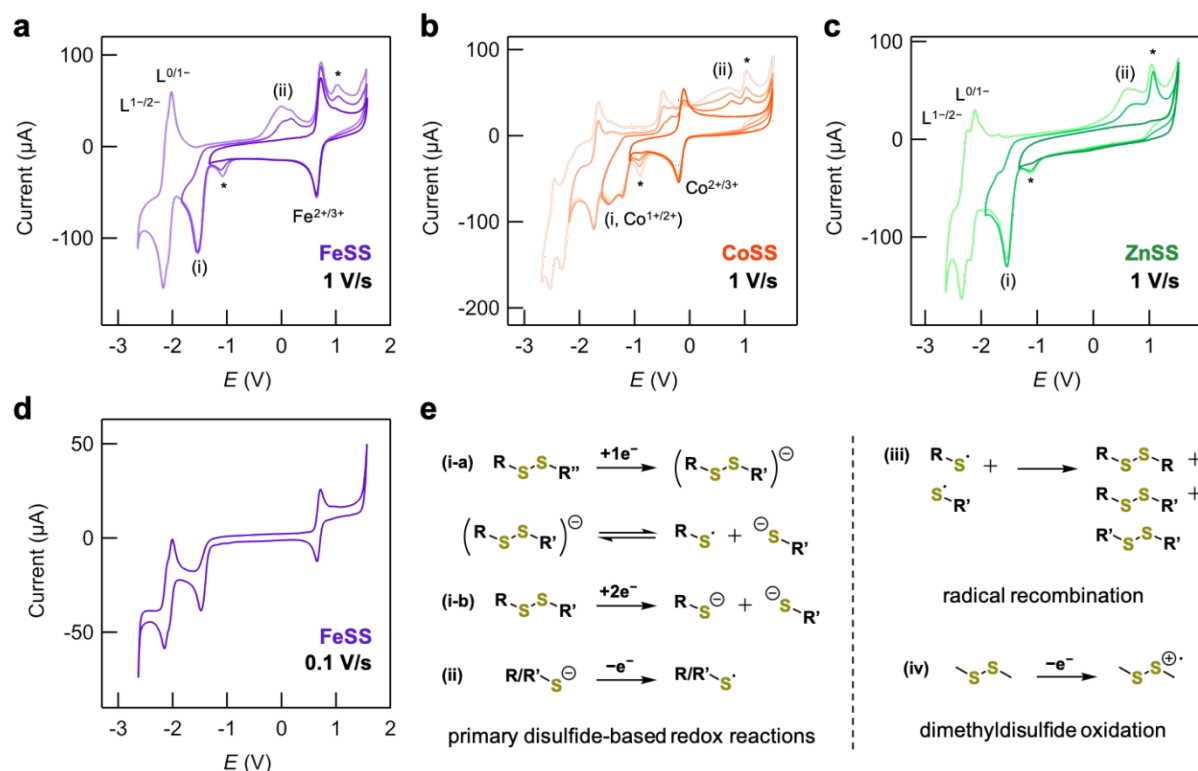


**Figure 3.** (a) Overlaid cyclic voltammograms of FeSS in MeCN–0.1 M <sup>n</sup>Bu<sub>4</sub>NPF<sub>6</sub>, extended to different reducing potentials. We tentatively attribute the new irreversible wave at –1.5 V (i), absent for the parent complex, to the 2 × 1 e<sup>−</sup> reduction of each disulfide group (see discussion). This reduction is associated with additional redox processes observed when scanning back to positive potentials. Here, (ii) labels mark features we associate with the thiolate oxidation processes shown in (e), “\*” indicates features we propose result from dimethyldisulfide oxidation (scheme (iv) in (e), voltammograms of dimethyldisulfide are shown in **Figure S3**). (b,c) Analogous overlaid cyclic voltammograms for CoSS and ZnSS. For CoSS, we observe that the Co<sup>2+/3+</sup> oxidation shifts from –0.109 to –0.486 mV after extension of the potential window to include disulfide reduction. It is to be expected that a complex bearing an electron-donating thiolate functionality (–S<sup>−</sup>; Hammett *para*-substituent constant, σ<sub>p</sub> = –1.21) would be more easily oxidized than the same complex with a –SSMe group (σ<sub>p</sub> = 0.13).<sup>41</sup> (d) A cyclic voltammogram of FeSS obtained at a slower scan rate (0.1 V/s). This shows that the additional redox processes and reactions associated with disulfide reduction are absent, confirming these originate from solution-based products that diffuse away from the electrode over extended timescales. (e) An overview of reaction schemes discussed in (a).

For all MSS complexes, we also observe a small irreversible oxidation feature ~1 V, commensurate with an irreversible reduction at ~–1V (waves marked “\*” in **Figure 3a-c**).



Notably, the potential of this oxidation feature is  $\sim$ constant and the same as that of an irreversible oxidation process in the voltammogram of **MeSSMe** (**Figure S3**, **Table S10**). We therefore attribute these events in voltammograms of **MSS** to oxidation of **MeSSMe** (scheme iv, **Figure 3e**; where **MeSSMe** is formed through recombination of two methylthiyl radicals) and reduction of the product(s) formed from its reactive radical cation. At slower scan rates the additional redox features associated with thiolate and **MeSSMe** oxidation are no longer observed in the voltammogram, confirming that they are associated with products of disulfide reduction that diffuse away from the electrode over extended timescales (**Figure 3d**). While identification of all electrochemically generated compounds is beyond the scope of this work, we note that the products formed from reactions of disulfide radical cations are considered dependent on the electrolyte, solvent, or impurities present. Reported species include: trisulfides ( $[\text{R}_3\text{S}_3]^+$ ), following disulfide radical dimerization to a  $[\text{R}_4\text{S}_4]^{2+}$  intermediate that subsequently undergoes nucleophilic attack by a neutral disulfide;<sup>42</sup> and protonated amides ( $\text{RSN}^+\text{H}_2\text{C}(\text{O})\text{CH}_3$ ), after reaction of  $[\text{RS}]^+$  with MeCN solvent and adventitious water.<sup>43</sup>

Further examination of the disulfide reduction and  $\text{M}^{2+/3+}$  oxidation features for **FeSS** shows that the ratio of their peak areas is  $\sim$ 2:1. This suggests that each disulfide undergoes a  $1\text{ e}^-$  reduction, or that a  $2\text{ e}^-$  reduction takes place at only one of the disulfide groups on this complex. For **FeSS** the difference between the peak and half-peak potentials ( $E_p - E_{p/2} = 56.5/n$ , where  $n$  is the number of electrons in the redox process) for the  $\text{Fe}^{2+/3+}$  wave is  $\sim$ 65 mV, close to the expected value for a  $1\text{ e}^-$  process.<sup>44</sup> However, for **FeSS** and **ZnSS** the disulfide reduction wave has  $E_p - E_{p/2} = 103$  and 94 mV, respectively. This peak broadening suggests the feature corresponds to two closely overlapping  $1\text{ e}^-$  processes, rather than a concerted  $2\text{ e}^-$  reduction. Accordingly, we tentatively assign this feature to the  $1\text{ e}^-$  reduction of each disulfide group, with the first and second reductions occurring at different potentials given that it is energetically more favorable to add an electron to a complex having a charge of  $2+$  than  $1+$ . Further evidence for this assignment may be provided in subsequent studies of related compounds, for example, through the electrochemical characterization of a heteroleptic complex comprising a single disulfide group. We note that for **CoSS** the disulfide reduction and  $\text{Co}^{1+/2+}$  features are convoluted, which severely complicates their analysis.

To evaluate the capability of **MSS** to form SAMs on gold, we exposed mechanically polished gold disc electrodes to 1 mM solutions of **FeSS** and **CoSS** in MeCN for  $\geq 18$  h. In **Figure 4b**, we present overlaid representative surface cyclic voltammograms for these electrodes measured in  $\text{CH}_2\text{Cl}_2$ -0.1 M  $^n\text{Bu}_4\text{NPF}_6$ . In each case, reversible redox features indicative of adsorbed **MSS** are clearly observed at potentials  $\sim$ 50-140 mV positive of the

potential of the corresponding  $M^{2+/3+}$  couple measured in solution (overlaid solution voltammograms are provided in **Figure 4a** for comparison;  $i_{pa}/i_{pc}$  close to 1 for redox active SAMs,  $i_p \propto V_s$ ; selected data is provided in the **SI, Table S11**). A comparable voltammetric response is observed for **CoSS** SAMs prepared on thermally evaporated gold electrodes, indicating the electrochemical properties and surface composition of these SAMs is broadly independent of the electrode surface roughness (**SI, Figure S4a**). The characteristic double-layer capacitance of **MSS** SAMs is lower than that suggested by the voltammograms in **Figure 3b**, as can be seen for voltammograms obtained from the same electrode when scanning to potentials below the oxidative limit (**SI, Figure S4b**). Similar surface voltammograms are observed for **CoSH** and **CoSS** SAMs prepared under an inert atmosphere (**Figure 4c**), indicating monolayers of comparable surface coverage and structure are formed using either –SH or –SSMe functionalized precursors. This result clearly shows that the use of –SSMe groups, despite generating surface adsorbed –SMe, does not impede the adsorption of these terpyridine complexes on gold electrodes.

We find that the intensity of  $M^{2+/3+}$  features for **MSS** SAMs does not significantly decrease upon repeated potential cycling, or after immersion in  $CH_2Cl_2/MeCN$  for 1 h, showing that these systems are broadly stable with respect to electrochemical characterization and solvent environment (**SI, Figure S5**). For completeness, we note that SAMs formed from an ostensibly pure **CoSS** sample prepared from  $Co(OAc)_2 \cdot 4H_2O$  (**SI, method A**; not subjected to chromatographic purification) often exhibited an unusual irreversible redox feature in surface voltammograms that disappeared after  $\sim 50$  potential cycles (**SI, Figure S4c**;  $E_{pa} \sim 1-1.2$  V). While the origin of this feature remains unclear, it is practically undetectable for **CoSS** SAMs prepared from  $CoCl_2 \cdot 6H_2O$  (**SI, method B**; subjected to a chromatographic purification step) and is typically not observed for SAMs formed from **CoSH**, **FeSS**, or **ZnSS**. Equilibrium cyclic voltammograms for SAMs comprising **CoSS** are presented unless otherwise stated. The saturation surface coverages ( $\Gamma \sim 34-52$  pmol/cm<sup>2</sup>), and full width half maximum for surface voltametric peaks ( $E_{FWHM} \sim 180-230$  mV) determined for the **MSS** (M = Fe, Co) SAMs studied here are consistent with reported values for other SAMs comprising charged polypyridyl complexes (**SI, Table S11**).<sup>3,7,45</sup> It has been suggested that the positive shift in the  $M^{2+/3+}$  redox potential upon surface binding, lower  $\Gamma$  than predicted for a close-packed monolayer, and greater  $E_{FWHM}$  than the 90 mV expected for non-interacting sites is due to repulsive intermolecular interactions within the adsorbed charged layer.<sup>45</sup>

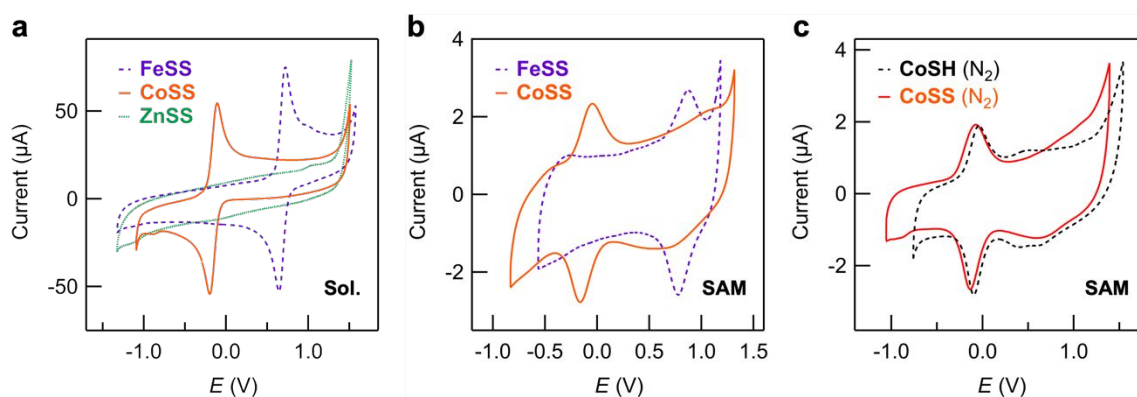


**Figure 4.** (a) Overlaid solution cyclic voltammograms for **MSS** where M = Fe (purple dashed), Co (orange solid), Zn (green dotted), reproduced from **Figure 3a-c** for convenience. Here the potential window is maintained above  $-1.4$  V vs. the  $\text{FcH}/[\text{FcH}]^+$  redox couple to avoid irreversible reduction of the disulfide group. (b) Overlaid representative surface cyclic voltammograms for **FeSS** and **CoSS** SAMs on gold measured over a potential window similar to that used in (a). For each SAM a single redox feature is observed close to the potential of the corresponding  $\text{M}^{2+/3+}$  couple measured in solution, indicating that the complex is attached to the surface. (c) Overlaid cyclic voltammograms obtained for **CoSH** (black dashed) and **CoSS** (orange solid) SAMs prepared under a nitrogen atmosphere in a glovebox. Redox features exhibit similar peak intensities and widths (taking into account electrode-electrode variation) indicating that SAMs of comparable structure and composition are formed from  $-\text{SH}$  and  $-\text{SSMe}$  functionalized precursors.

## CONCLUSION

In this work we have demonstrated that metal bis(terpyridine) complexes comprising directly connected  $-\text{SSMe}$  groups are stable in aerated solution, and with respect to electrochemical potentials as low as  $\sim -1.4$  V vs.  $\text{FcH}/[\text{FcH}]^+$ . We further show that these **MSS** complexes can be used to form SAMs with comparable electrochemical properties to those formed from **CoSH**. It is anticipated that this unconventional protecting group strategy may also prove useful for the installation and utility of stable surface-binding sulfur groups on other compounds, particularly those comprising counterions or prone to decomposition in basic media. We find that **CoSH** is air sensitive in solution, and caution that it must be handled and studied with care to avoid complications arising from its rapid decomposition. Taken together, this work provides a firm basis for subsequent studies focused on single- and multi-component functionalization of metal surfaces using **MSS** precursors, or chemisorbed gold-sulfur linked **MSS** single-molecule junctions.

## ASSOCIATED CONTENT

Electronic Supplementary Information (ESI) available: Additional experimental details, synthetic, crystallographic, and electrochemical data,  $^1\text{H}$  and  $^{13}\text{C}\{^1\text{H}\}$  NMR spectra for all new compounds.

## AUTHOR INFORMATION

### Corresponding Author

Michael S. Inkpen – Email: [inkpen@usc.edu](mailto:inkpen@usc.edu)

### Notes

The authors declare no competing financial interest.

## ACKNOWLEDGEMENTS

Acknowledgement is made to the donors of the American Chemical Society Petroleum Research Fund (62751-DNI5), and University of Southern California (USC) startup funds, for support of this research. We thank Nils Rotthowe for useful discussions, and are grateful to the NSF (DBI-0821671, CHE-0840366, CHE-1048807, CHE-2018740) and the NIH (S10 RR25432) for analytical instrumentation.

## REFERENCES

1. Park, J., Pasupathy, A. N., Goldsmith, J. I., Chang, C., Yaish, Y., Petta, J. R., Rinkoski, M., Sethna, J. P., Abruña, H. D., McEuen, P. L. & Ralph, D. C. Coulomb blockade and the Kondo effect in single-atom transistors. *Nature* **417**, 722–725 (2002).
2. Parks, J. J., Champagne, A. R., Costi, T. A., Shum, W. W., Pasupathy, A. N., Neuscamman, E., Flores-Torres, S., Cornaglia, P. S., Aligia, A. A., Balseiro, C. A., Chan, G. K. L., Abruña, H. D. & Ralph, D. C. Mechanical control of Spin States in Spin-1 Molecules and the Underscreened Kondo Effect. *Science* **328**, 1370–1373 (2010).
3. Gang, T., Yilmaz, M. D., Ataç, D., Bose, S. K., Strambini, E., Velders, A. H., De Jong, M. P., Huskens, J. & Van Der Wiel, W. G. Tunable doping of a metal with molecular spins. *Nature Nanotechnol.* **7**, 232–236 (2012).
4. Seo, K., Konchenko, A. V., Lee, J., Gyeong, S. B. & Lee, H. Molecular conductance switch-on of single ruthenium complex molecules. *J. Am. Chem. Soc.* **130**, 2553–2559 (2008).
5. Baisch, B., Raffa, D., Jung, U., Magnussen, O. M., Nicolas, C., Lacour, J., Kubitschke, J. & Herges, R. Mounting freestanding molecular functions onto surfaces: The

- platform approach. *J. Am. Chem. Soc.* **131**, 442–443 (2009).
6. Dong, T.-Y., Huang, C., Chen, C.-P. & Lin, M.-C. Molecular self-assembled monolayers of ruthenium(II)-terpyridine dithiol complex on gold electrode and nanoparticles. *J. Organomet. Chem.* **692**, 5147–5155 (2007).
  7. Campagnoli, E., Hjelm, J., Milios, C. J., Sjodin, M., Pikramenou, Z. & Forster, R. J. Adsorption dynamics and interfacial properties of thiol-based cobalt terpyridine monolayers. *Electrochim. Acta* **52**, 6692–6699 (2007).
  8. Murphy, F. A., Suarez, S., Figgemeier, E., Schofield, E. R. & Draper, S. M. Robust self-assembled monolayers of Ru<sup>II</sup> and Os<sup>II</sup> polypyridines on gold surfaces: Exploring new potentials. *Chem. Eur. J.* **15**, 5740–5748 (2009).
  9. Lee, J., Chang, H., Kim, S., Bang, G. S. & Lee, H. Molecular monolayer nonvolatile memory with tunable molecules. *Angew. Chem. Int. Ed.* **48**, 8501–8504 (2009).
  10. Nováková Lachmanová, Š., Vavrek, F., Sebechlebská, T., Kolivoška, V., Valášek, M. & Hromadová, M. Charge transfer in self-assembled monolayers of molecular conductors containing tripodal anchor and terpyridine-metal redox switching element. *Electrochim. Acta* **384**, (2021).
  11. Liatard, S., Chauvin, J., Balestro, F., Jouvenot, D., Loiseau, F. & Deronzier, A. An Original Electrochemical Method for Assembling Multilayers of Terpyridine-Based Metallic Complexes on a Gold Surface. *Langmuir* **28**, 10916–10924 (2012).
  12. Nerngchamng, N., Thompson, D., Cao, L., Yuan, L., Jiang, L., Roemer, M. & Nijhuis, C. A. Nonideal Electrochemical Behavior of Ferrocenyl–Alkanethiolate SAMs Maps the Microenvironment of the Redox Unit. *J. Phys. Chem. C* **119**, 21978–21991 (2015).
  13. Maskus, M. & Abruña, H. D. Synthesis and Characterization of Redox-Active Metal Complexes Sequentially Self-Assembled onto Gold Electrodes via a New Thiol–Terpyridine Ligand. *Langmuir* **12**, 4455–4462 (1996).
  14. Tuccitto, N., Ferri, V., Cavazzini, M., Quici, S., Zhavnerko, G., Licciardello, A. & Rampi, M. A. Highly conductive ~40-nm-long molecular wires assembled by stepwise incorporation of metal centres. *Nature Mater.* **8**, 41 (2008).
  15. Sakamoto, R., Wu, K.-H., Matsuoka, R., Maeda, H. & Nishihara, H.  $\pi$ -Conjugated bis(terpyridine)metal complex molecular wires. *Chem. Soc. Rev.* **44**, 7698–7714 (2015).
  16. Tang, J., Wang, Y., Klare, J. E., Tulevski, G. S., Wind, S. J. & Nuckolls, C. Encoding molecular-wire formation within nanoscale sockets. *Angew. Chem. Int. Ed.* **46**, 3892–

- 3895 (2007).
17. Sullivan, T. P. & Huck, W. T. S. Reactions on Monolayers: Organic Synthesis in Two Dimensions. *European J. Org. Chem.* **2003**, 17–29 (2003).
  18. Poisson, J., Geoffrey, H. L., Ebralidze, I. I., Laschuk, N. O., Allan, J. T. S., Deckert, A., Easton, E. B. & Zenkina, O. V. Layer-by-Layer Assemblies of Coordinative Surface-Confined Electroactive Multilayers: Zigzag vs Orthogonal Molecular Wires with Linear vs Molecular Sponge Type of Growth. *J. Phys. Chem. C* **122**, 3419–3427 (2018).
  19. Inkpen, M. S., Leroux, Y. R., Hapiot, P., Campos, L. M. & Venkataraman, L. Reversible on-surface wiring of resistive circuits. *Chem. Sci.* **8**, 4340–4346 (2017).
  20. Van Der Geer, E. P. L., Van Koten, G., Klein Gebbink, R. J. M. & Hessen, B. A. [4Fe-4S] cluster dimer bridged by bis(2,2':6',2''-terpyridine-4'-thiolato)iron(II). *Inorg. Chem.* **47**, 2849–2857 (2008).
  21. Silva, M. J. J. P., Bertocello, P., Daskalakis, N. N., Spencer, N., Kariuki, B. M., Unwin, P. R. & Pikramenou, Z. Surface-active mononuclear and dinuclear Ru(II) complexes based on thio-substituted terpyridines bearing cyclodextrin recognition units. *Supramol. Chem.* **19**, 115–127 (2007).
  22. Kuehnel, M. F., Orchard, K. L., Dalle, K. E. & Reisner, E. Selective Photocatalytic CO<sub>2</sub> Reduction in Water through Anchoring of a Molecular Ni Catalyst on CdS Nanocrystals. *J. Am. Chem. Soc.* **139**, 7217–7223 (2017).
  23. Wen, H.-M., Zhang, D.-B., Zhang, L.-Y., Shi, L.-X. & Chen, Z.-N. Efficient Synthetic Approaches To Access Ruthenium(II) Complexes with 2-(Trimethylsilyl)ethyl- or Acetyl-Protected Terpyridine–Thiols. *Eur. J. Inorg. Chem.* **2011**, 1784–1791 (2011).
  24. Bain, C. D., Biebuyck, H. A. & Whitesides, G. M. Comparison of self-assembled monolayers on gold: coadsorption of thiols and disulfides. *Langmuir* **5**, 723–727 (1989).
  25. Inkpen, M. S., Liu, Z., Li, H., Campos, L. M., Neaton, J. B. & Venkataraman, L. Non-chemisorbed gold–sulfur binding prevails in self-assembled monolayers. *Nature Chem.* **11**, 351–358 (2019).
  26. Horikoshi, R. & Mochida, T. Metal complexes of 4,4'-dipyridyldisulfide-structural diversity derived from a twisted ligand with axial chirality. *Coord. Chem. Rev.* **250**, 2595–2609 (2006).
  27. Constable, E. C., Hermann, B. A., Housecroft, C. E., Neuburger, M., Schaffner, S. & Scherer, L. J. 2,2':6,2''-Terpyridine-4'(1'H)-thione: A missing link in

- metallo-supramolecular chemistry. *New J. Chem.* **29**, 1475–1481 (2005).
28. Heister, K., Allara, D. L., Bahnck, K., Frey, S., Zharnikov, M. & Grunze, M. Deviations from 1:1 compositions in self-assembled monolayers formed from adsorption of asymmetric dialkyl disulfides on gold. *Langmuir* **15**, 5440–5443 (1999).
  29. Bain, C. D. & Whitesides, G. M. Formation of monolayers by the coadsorption of thiols on gold: Variation in the length of the alkyl chain. *J. Am. Chem. Soc.* **111**, 7164–7175 (1989).
  30. Porter, M. D., Bright, T. B., Allara, D. L. & Chidsey, C. E. D. Spontaneously organized molecular assemblies. 4. Structural characterization of n-alkyl thiol monolayers on gold by optical ellipsometry, infrared spectroscopy, and electrochemistry. *J. Am. Chem. Soc.* **109**, 3559–3568 (1987).
  31. Kitson, T. M. & Loomes, K. M. Synthesis of methyl 2- and 4-pyridyl disulfide from 2- and 4-thiopyridone and methyl methanethiosulfonate. *Anal. Biochem.* **146**, 429–430 (1985).
  32. Harzmann, G. D., Neuburger, M. & Mayor, M. 4,4''-Disubstituted Terpyridines and their Homoleptic Fe<sup>II</sup> Complexes. *Eur. J. Inorg. Chem.* **2013**, 3334–3347 (2013).
  33. Constable, E. C., Housecroft, C. E., Kulke, T., Lazzarini, C., Schofield, E. R. & Zimmermann, Y. Redistribution of terpy ligands—approaches to new dynamic combinatorial libraries. *J. Chem. Soc. Dalton Trans.* 2864–2871 (2001).
  34. Gryko, D. T., Clausen, C., Roth, K. M., Dontha, N., Bocian, D. F., Kuhr, W. G. & Lindsey, J. S. Synthesis of ‘Porphyrin-linker-thiol’ molecules with diverse linkers for studies of molecular-based information storage. *J. Org. Chem.* **65**, 7345–7355 (2000).
  35. Chow, H. S., Constable, E. C., Housecroft, C. E., Kulicke, K. J. & Tao, Y. When electron exchange is chemical exchange—assignment of <sup>1</sup>H NMR spectra of paramagnetic cobalt(II)-2,2':6',2''-terpyridine complexes. *Dalton Trans.* 236–237 (2005).
  36. Miao, Z., Quainoo, T., Czyszczon-Burton, T. M., Rotthowe, N., Parr, J. M., Liu, Z. & Inkpen, M. S. Charge transport across dynamic covalent chemical bridges. *Nano Lett.* **22**, 8331–8338 (2022).
  37. Borsari, M., Cannio, M. & Gavioli, G. Electrochemical behavior of diphenyl disulfide and thiophenol on glassy carbon and gold electrodes in aprotic media. *Electroanalysis* **15**, 1192–1197 (2003).
  38. Widrig, C. A., Chung, C. & Porter, M. D. The electrochemical desorption of n-alkanethiol monolayers from polycrystalline Au and Ag electrodes. *J. Electroanal.*

- Chem. Interfacial Electrochem.* **310**, 335–359 (1991).
39. Maran, F., Wayner, D. D. M. & Workentin, M. S. *Kinetics and mechanism of the dissociative reduction of C–X and X–X bonds (X = O, S). Advances in Physical Organic Chemistry* vol. 36 (2001).
  40. Hall, G. B., Kottani, R., Felton, G. A. N., Yamamoto, T., Evans, D. H., Glass, R. S. & Lichtenberger, D. L. Intramolecular electron transfer in bipyridinium disulfides. *J. Am. Chem. Soc.* **136**, 4012–4018 (2014).
  41. Hansch, C., Leo, A. & Taft, R. W. A survey of Hammett substituent constants and resonance and field parameters. *Chem. Rev.* **91**, 165–195 (1991).
  42. Lam, K. & Geiger, W. E. Anodic Oxidation of Disulfides: Detection and Reactions of Disulfide Radical Cations. *J. Org. Chem.* **78**, 8020–8027 (2013).
  43. Bewick, A., Coe, D. E., Libert, M. & Mellor, J. M. Mechanism of anodic acetamidophilenylation and acetamidoseleation of alkenes. *J. Electroanal. Chem.* **144**, 235–250 (1983).
  44. Bard, A. J. & Faulkner, L. Y. *Electrochemical Methods*. (Wiley, 2004).
  45. Figgemeier, E., Merz, L., Hermann, B. A., Zimmermann, Y. C., Housecroft, C. E., Gu, H.-J. & Constable, E. C. Self-Assembled Monolayers of Ruthenium and Osmium Bis-Terpyridine Complexes Insights of the Structure and Interaction Energies by Combining Scanning Tunneling Microscopy and Electrochemistry. *J. Phys. Chem. B* **107**, 1157–1162 (2003).



